

SOLAR SAIL STARSHIPS: THE CLIPPER SHIPS OF THE GALAXY

Journal of the British Interplanetary Society, Vol. 34, pp. 371-380, 1981.

GREGORY L. MATLOFF*

Department of Applied Science, New York University, 26-36 Stuyvesant Street, New York, New York 10003, USA.

* Currently on leave of absence with the Systems and Applied Sciences Corporation, Riverdale, Md. 10840, USA.

EUGENE MALLOVE

Astronomy New England, 215 Highland Street, Holliston, Mass. 07146, USA.

The utility of 10^{-8} - 10^{-7} meter (m) thick space manufactured solar sails for interstellar mission launch is considered. An interstellar solar sail is assumed to be partially or completely deployed behind a much more massive chunk of asteroidal debris with similar dimensions to the sail and utilized as an occulter. The sail is released from the occulter and exposed to sunlight, during a 1.5×10^9 m perihelion pass in a near-parabolic or hyperbolic orbit. Robot probes would be deposited as thin films on the spaceward side of the sails; larger habitats with human crews would be suspended by diamond or copper cables behind the sails. Stress problems in the cable and sail, the applicability of giant-planet rebounds, sail deployment strategies, thermal problems and preliminary mission design are all considered. Near term technology may be capable of launching small robot probes that could reach Alpha Centauri within about 350 years. Much larger human-occupied habitats, constrained to lower peak accelerations, may eventually be able to utilize the solar sail to reach Alpha Centauri within 900-1400 years. Eventually, when our Sun enters its giant phase about 4×10^9 years in the future, the performance of the solar sail as an interstellar booster will greatly increase.

1. INTRODUCTION

ALTHOUGH THEORETICAL ANALYSIS of solar sails have been performed for several decades [1] this propulsion system required several advances in materials science before it could be considered for interplanetary missions. Recently state-of-the-art solar sails were considered to propel the 1986 Haley's comet probe [2] and more advanced space-manufactured sails are now under consideration for application to space industrialization and colonization [3].

The use of solar sails for expeditions into interstellar space has not yet been subjected to detailed analysis, but sails have been proposed as receivers of beamed laser energy for interstellar missions [4, 5]. Forward has suggested that thin-film remote probes might be deposited on the spaceward side of very thin solar sails, which would use the gravity whip principle and solar sail deployment near the Sun, for interstellar boosting [6]. Viewing et al speculated that solar sail boosted "innocuous starships" from other civilizations might, for reasons of economy, be more prevalent in the Galaxy than the much faster ships using thermonuclear or antimatter propulsion [7].

Interstellar missions utilizing the solar sail will be length) A large space colony, suspended by diamond sails behind a solar sail, would be, constrained by human acceleration tolerance and sail/cable stressing, to interstellar flight times of about 1000 years.

Such long transit times may not be unreasonable because automated, miniaturized scientific probes with great long longevity may eventually become feasible [6] and mobile space habitats such as those proposed by O'Neill may be sociologically reliable enough to withstand long interstellar journeys [8]. Also, if we evolve into a solar-system-wide civilization which survives for some four billion years, conditions for solar-sailing will improve and will drastically

reduce interstellar flight times, when the Sun becomes a red giant star [9]. As described below, the solar sail may indeed be the "appropriate technology" to allow a Type II civilization [10] to escape the dire consequences of it expanding parent star.

In the sections below, sail kinematics, stressing, deployment strategies, aspects of mission design, interstellar cruise, and deceleration will be considered. We will first consider the kinematics of fully and partially deployed solar sails.

2. SOLAR SAIL KINEMATICS

Figure 1 presents a solar-sail/payload configuration for thin-film robot probes and mobile habitats.

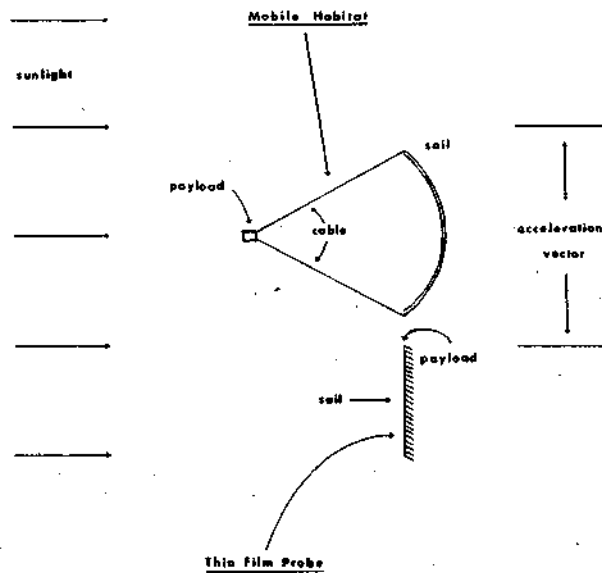


Fig. 1. Solar Sail, Cable, and Payload Arrangement.

In Fig. 2, we present a possible method of sail deployment near the Sun.

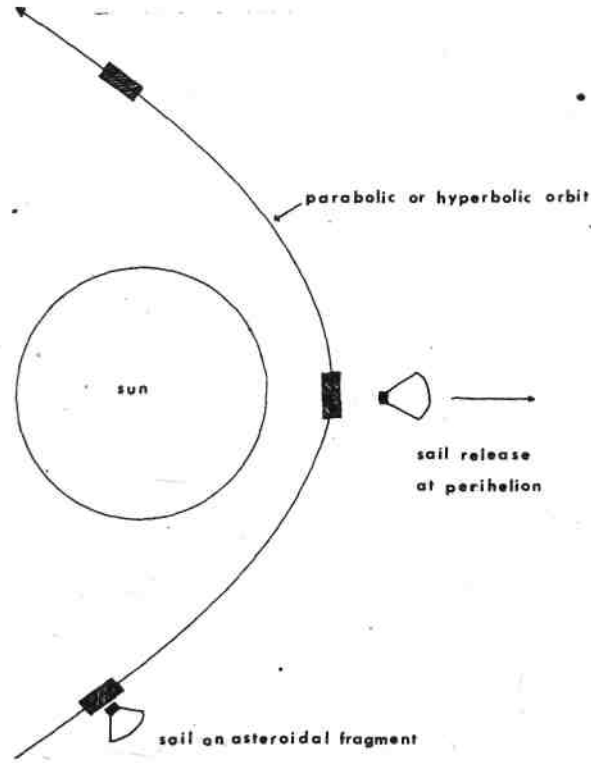


Fig. 2. Use of an Asteroidal Launching Pad or Occulter to Deploy Sail Near the Sun.

The sail, either partially or completely unfurled, is manoeuvred into a parabolic or hyperbolic orbit with a perihelion approach 0.01-0.03 AU from the Sun's centre. The sail is deployed behind a much more massive occulter of similar dimension which is discarded at perihelion. According to Ehrlicke, a 0.01 AU perihelion approach is the closest feasible [11]. For a near parabolic orbit, the perihelion velocity $V_0 \leq \sqrt{2} * V_{\text{circ}}$, where V_{circ} is the velocity required to maintain a circular orbit at the perihelion distance. For $r_0 = 0.01$ AU, $V_0 \leq 0.0014$ C, for $r_0 = 0.03$ AU, $V_0 \leq 0.0008$ C. If an 18-24 km/sec manoeuvre is performed near Saturn, the hyperbolic velocity at $r_0 = 0.01$ AU will be $V_0 \approx 0.002$ C, relative to the Sun [11].

For the probe and habitat boosting systems shown in Fig. 1, the total mass at time of occulter release can be expressed for a sail of circular cross section:

$$\begin{aligned}
 M_{\text{probe}} &= M_{\text{sail}} + M_{\text{payload}} = \pi (\sigma_s + \sigma_{pa}) R_s^2 \\
 M_{\text{habitat}} &= M_{\text{sail}} + M_{\text{cable}} + M_{\text{payload}} \\
 &= \pi \sigma_s R_s^2 + \rho_c L_c A_c + M_p,
 \end{aligned} \tag{1}$$

where σ_s is the sail areal mass loading (kg/m^2), σ_{pa} is the thin-film probe's areal mass loading (kg/m^2), R_s (m) is sail radius (cross-sectional radius presented to Sun), ρ_c (kg/m^3) is the cable material density, L_c (m) is the cable length ($L_c > R_s$, as shown below), A_c (m^2) is the total cable cross-sectional area, and M_p is the payload mass in kg.

Using the inverse-square law, solar irradiance on a sail at a distance r from the centre of the Sun, normal to the Sun is:

$$S_r = \frac{1.35 \times 10^3 (1.5 \times 10^{11})^2}{r^2} = \frac{3.04 \times 10^{25}}{r^2} \text{ watt/m}^2 \tag{2}$$

(All quantities in this paper are in S. I. system units unless otherwise specified).

From Tsu [1] for a sail of 100% reflectivity the radiation pressure can be written $2S_r/C$, where C is the speed of light. For sail reflectivity k , the solar radiation pressure can be written $[(1+k)/2] S_r/C$. Thus, a 95% sail reflectivity will reduce the solar radiation pressure by 2.5%. Therefore, the radial acceleration of the spacecraft due to solar radiation pressure can be written.

$$\bar{V}_s = \left(\frac{1+k}{2}\right) \frac{6.3 \times 10^{17} R_s^2}{Mr^2} \text{ m/sec}^2 \quad (3)$$

From elementary conservation of energy, the solar sail's velocity V at distance r from the Sun's centre is given by:

$$\frac{V^2}{2} - \frac{GM_\odot}{r} = \frac{V_0^2}{2} - \frac{GM_\odot}{r_0} + \int_{r_0}^r \left(\frac{1+k}{2}\right) \frac{6.3 \times 10^{17} R_s^2}{Mr^2} dr \quad (4)$$

where G is the gravitational constant, M_\odot is the mass of the Sun, and the "0" subscripts denote initial conditions. Two assumptions made in Eq. (4) are that the sail axis will always be directed toward the Sun and the sail is fully deployed between r_0 and r . The solar sail's hyperbolic excess velocity, V_∞ is obtained from Eq. (4) by letting r go to infinity:

$$V_\infty = \left[\frac{\left(\frac{1+k}{2}\right) 1.26 \times 10^{18} R_s^2 - 2.66 \times 10^{28} M}{Mr_0} + V_0^2 \right]^{1/2} \text{ m/sec} \quad (5)$$

We can analyze the performance of large solar sails by defining an effective mass thickness or areal density, σ_e , for the sail/thin-film payload, or sail/cable/payload combination. From Eq. (5),

$$\sigma_e = \frac{M}{\pi R_s^2} = \frac{\left(\frac{1+k}{2}\right) 4.01 \times 10^{17}}{r_0 V_\infty^2 - r_0 V_0^2 + 2.66 \times 10^{20}} \text{ kg/m}^2 \quad (6)$$

Using Eq. (3), the maximum spacecraft acceleration can be related to σ_e :

$$V_{s \text{ max}} = \left(\frac{1+k}{2}\right) \frac{2 \times 10^{17}}{r_0^2 \sigma_e} \text{ m/sec}^2 \quad (7)$$

Drexler has reported that a 10^{-7} m thickness will certainly be possible for space manufactured solar sails and that there is some possibility of producing sails as thin as 10^{-8} m [3]. Tsu projects sail material specific gravity to be 1.18 [1]. Table 1 presents solutions to Eqs: (6) and (7) for a variety of final velocities and perihelion velocities. For simplicity, sail reflectivities were assumed to be 100%, in preparing Table 1.

TABLE 1. Performance of Solar Sails Fully Deployed at Perihelion: V_∞ = velocity at infinity, V_0 = velocity at perihelion, C = speed of light, σ_e = effective mission mass area loading, $V_{s \text{ max}}$ = maximum acceleration.

V_∞ / C	V_0 / C	σ_e (kg/m ²)	$V_{s \text{ max}}$ (g _{earth})
0.0014	0.0014	1.51×10^{-3}	6.02
0.002	- " -	7.40×10^{-4}	12.75
0.003	- " -	3.30×10^{-4}	27.51
0.004	- " -	1.86×10^{-4}	48.89
0.005	- " -	1.19×10^{-4}	76.37
0.007	- " -	6.06×10^{-5}	149.65
0.009	- " -	3.67×10^{-5}	247.37

0.011.	- " -	2.45×10^{-5}	369.51
0.012	- " -	2.06×10^{-5}	439.00
0.013	- " -	1.76×10^{-5}	516.09
0.015	- " -	1.32×10^{-5}	687.09
0.002	0.002	1.51×10^{-3}	6.02
0.003	- " -	4.26×10^{-4}	21.28
0.004	- " -	2.13×10^{-4}	42.62
0.005	- " -	1.29×10^{-4}	70.14
0.007	- " -	6.32×10^{-4}	143.42
0.009	- " -	3.76×10^{-5}	241.14
0.011	- " -	2.50×10^{-5}	363.29
0.013	- " -	1.78×10^{-5}	509.86
0.015	- " -	0.33×10^{-5}	680.86

In evaluating Table 1, it is worth noting that, at 0.01 AU, from the Sun, the gravitational acceleration of the Sun is $6.01 g_{\text{earth}}$, where g_{earth} is Earth's surface gravity. Although human beings have withstood as much as $45 g_{\text{earth}}$ for fractions of a second, the record for extended high acceleration without ill effects or loss of consciousness is $17 g_{\text{earth}}$ for four minutes [12,13]. Thus, even with planetary rebounds and a 18-74 km/sec powered peri-Saturn manoeuvre for $V_0 = 0.002 C$, the fully-deployed sail for use in transporting a human-occupied space habitat seems limited to $V_\infty \leq 0.003 C$, extrapolating well past this $17 g_{\text{earth}}$ limit.

To further consider the kinematics of a sail-launched interstellar habitat, we will constrain solar sail radius such that the astronauts never experience more than a given acceleration. This could be accomplished by requiring $R_s/r = \text{constant}$, near the Sun. Further out, after maximum solar sail deployment, $R_s = \text{constant}$. The acceleration experienced by the crew is expressed in Eq. (3) and the acceleration of the spacecraft relative to the Sun can be calculated by subtracting the gravitational acceleration towards the Sun from Eq. (4).

Calling the maximum allowable acceleration V_A [с точкой, dt] and utilizing $R_s/r = \text{constant}$ and Eq. (3),

$$R_s^2/r^2 = [V_A M / (6.3 \times 10^{27})] \left[\frac{2}{1+k} \right], \quad (8)$$

during the initial acceleration period. We next define $V_p = \text{velocity at perihelion (start of sail deployment)}$, $r_p = \text{perihelion distance}$. Once again, $V_0 = \text{velocity at the time of sail full deployment}$, and $r_0 = \text{distance from the Sun's centre to the position at which the sail is fully deployed}$. Now, since $V[\text{с точкой, dt}] = V dv/dr$,

$$\int_{V_p}^{V_0} V_s dV_s = \int_{r_p}^{r_0} V_A dr - \int_{r_p}^{r_0} \frac{1.33 \times 10^{20}}{r^2} dr$$

since $GM_0 = 1.33 \times 10^{20}$. Integrating, we can relate initial (perihelion) conditions to conditions at the start of "fully deployed sail" operations:

$$\frac{V_O^2}{2} - \frac{V_P^2}{2} = V_A (r_O - r_P) - 1.33 \times 10^{20} \left(\frac{1}{r_P} - \frac{1}{r_O} \right), \quad (10)$$

which leads to:

$$V_O = [2V_A (r_O - r_P) - 2.66 \times 10^{20} \left(\frac{r_O - r_P}{r_O r_P} \right) + V_P^2]^{1/2} \quad (11)$$

and, from Eq. (3),

$$r_O = \left[\frac{\left(\frac{1+\kappa}{2} \right) 6.3 \times 10^{17} R_s^2 F.S.}{V_A M} \right]^{1/2} \quad (12)$$

where $R_{s(F.S.)}$ is fully deployed sail radius.

Equation (11) and (12) can be used as input to Eq. (5), to relate V_∞ to initial conditions, at perihelion. Solutions to these equations, calculated for 100% sail reflectivity, are presented in Fig. 3 for several perihelion velocities and values of $\sigma_e = M/(\pi R_s^2)$. Note the variety of configurations capable of travelling to a Centauri in 800-1300 years, with accelerations limited to 10 or 20 g_{earth} .

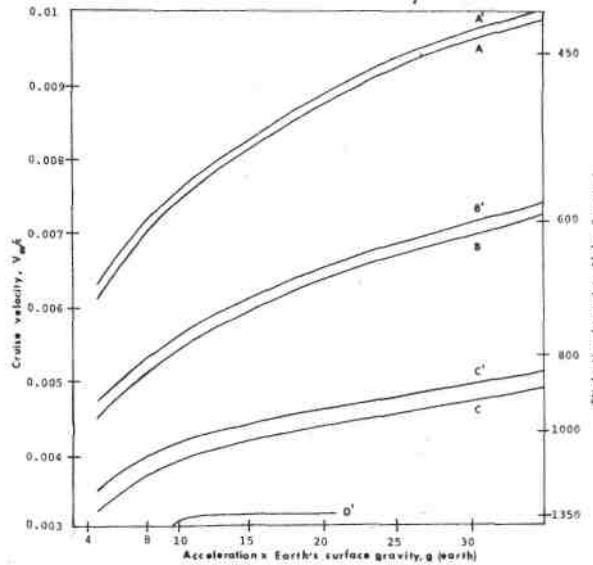


Fig. 3. Performance of an Interstellar Solar Starship that has a partially deployed sail at perihelion, which deploys such that $R_s/r = \text{constant}$ until full sail deployment. $R_s = \text{sail radius}$ and $r = \text{distance from Sun centre}$. Cases A, B, C, D respectively refer to mission effective mass thickness of 1.18×10^{-5} , 3.73×10^{-5} , 1.18×10^{-4} and 3.73×10^{-4} kg/m. Unprimed cases have perihelion velocity 0.0014 C, primed cases have perihelion velocity 0.002 C.

It is good for possible interstellar applications of the solar sail that effective mass loadings 3-10 times Drexler's minimum are capable of such performance, even without a powered peri-Saturn manoeuvre. Because, as will be shown in the following section, considerations of sail stress dynamics will add to the projected system mass.

3. STRESS ANALYSIS

In considering the stress dynamics of this interstellar propulsion system, we first consider the cables. We assume, as shown in Fig. 4, a cable length L_c , sail radius projected to the Sun, R_s ,

θ is the angle between the normal to the sail and the cable. Most stress is assumed to be taken up by cables joined to the circular sail's outer perimeter. If T_c is cable tension, F_s is the component of the cable tension balancing the sunlight pressure on the sail and F_R is the radial force on the sail, towards the sail centre.

$$\begin{aligned} \cos \theta &= F_s/T_c, \sin \theta = R_s/L_c, \text{ and} \\ (F_s/T_c)^2 &= 1 - \sin^2 \theta = 1 - (R_s/L_c)^2 \end{aligned} \quad (13)$$

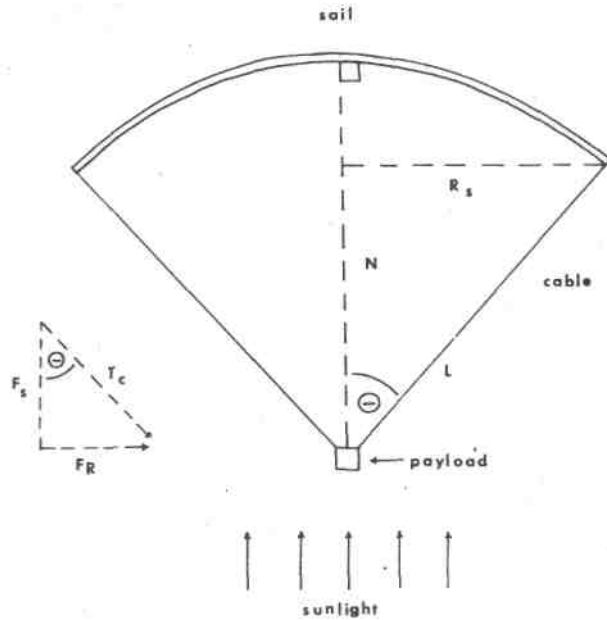


Fig. 4. Consideration of cable/sail stress: L - cable length, θ = angle between normal to sail (N) and cable, R_s = sail effective radius projected to Sun, T_c = cable tension, F_s = component of cable tension balancing sunlight pressure on sail, and F_R = radial force on sail. Force diagrams and mathematical (non-physical) constructs are in dotted lines.

We expect optimum operation for the condition $(F_s/T_c)^2 = 1/2$, $(R_s/L_c)^2 = 1/2$ which results in $(R_s/L_c) = 0.7$, $\theta = 45^\circ$, $T_c = 1.4 F_s$, $L_c = 1.4R$ and $F_R = F_s$.

Before considering the radial force on the sail canopy, which must be balanced unless the sail is very strong, some further details of cable design will be presented. Cable specific gravity will be written as ρ_c , and cable tensile strength is η . If cable total area is A_c , the peak force on the cables can be written:

$$F_{\text{peak}} = \dot{V}_{sA} (M_c + M_p) \leq A_c \eta, \quad (14)$$

where V_{sA} is maximum acceleration and, once again, M_c is total cable mass and M_p is payload mass. From Eq. (1), and the above discussion, $M_c = \rho_c L_c A_c = 1.4 \rho_c R_s A_c$. If diamond cables are used to establish an upper limit on materials performance, $\rho_c = 3.52 \times 10^3 \text{ kg/m}^3$, an $\eta = 5.3 \times 10^{10} \text{ Newton/m}^2$ [14]. Equation (14) can be rewritten:

$$M_c \geq \frac{1.4 \rho_c R_s M_p}{\frac{\eta}{\dot{V}_{sA}} - 1.4 \rho_c R_s} \quad (15)$$

which allows us to relate cable mass to payload mass, spacecraft acceleration, and sail radius. For the cable mass $M_c \geq M_p$, $\eta / V_{sA} = 2.4 \rho_c R_s$, for $M_c > 0.5 M_p$, $\eta / V_{sA} = 4.2 \rho_c R_s$, and for $M_c > 2.0 M_p$, $\eta / V_{sA} = 2.1 \rho_c R_s$. Equation (15) is solved for diamond and copper (for copper

$\rho_c = 8.52 \times 10^3 \text{ kg/m}^3$, $\eta = 3.71 \times 10^{10} \text{ Newton/m}^2$) [17] in Fig. 5, for accelerations of $6 g_{\text{earth}}$ and $10 g_{\text{earth}}$.

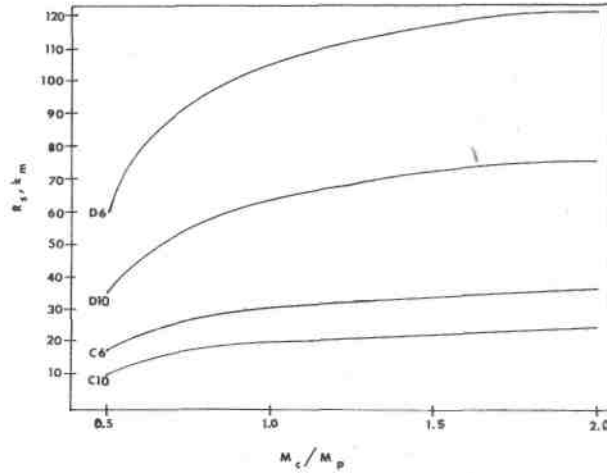


Fig. 5. Effective fully deployed sail radius for fully stressed cables, as a function of cable mass/payload mass (M_c/M_p), cable material (D - diamond; C = copper), and maximum acceleration Vs_A . Cases D6 and D10 are for diamond, $Vs_A = 6$, and $10 g_{\text{earth}}$, respectively. C6 and C10 present corresponding results for copper.

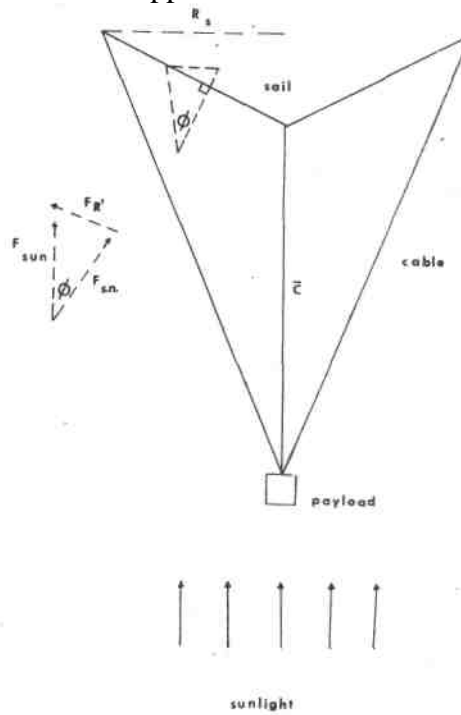


Fig. 6. Use of an Inward Tilted Solar Sail to Balance the radial component of cable tension. Angle θ is angle between solar radiation pressure F_{SUN} and its component normal to the sail, $F_{\text{S,N}}$. Central Cable C connects payload to sail centre. $F_{R'}$, is solar radiation pressure component radial to the sail.

We next consider F_R , the radial component of cable tension. There are two ways to balance this force component. One requires spinning the sail and the other requires tilting it inward, as shown in Fig. 6. A spinning sail, in which centrifugal force is used to balance F_R , will be considered first.

For a $\theta = 45^\circ$ sail angle, as in Fig. 4, $F_R = F_S$. Requiring centrifugal force to balance radial cable force component F_R , maximum sail spin velocity can be written:

$$V_{SPIN} = \left(\frac{M_c + M_p}{M_s} \dot{V}_{sA} R_s \right)^{1/2} \quad (16)$$

For the case $M_c = M_p$, $M_c + M_p = M_s$, and $V_{sA} = 10^4$ cm/sec² ($\approx 10 g_{\text{earth}}$). $V_{SPIN} \approx 10^2 R_s^{1/2}$. For a 10 km radius sail, $V_{SPIN} \approx 1$ km/sec and for a 100 km radius sail, $V_{SPIN} \approx 3$ km/sec. The kinetic energy of the rotating sail can be written [15]:

$$\begin{aligned} \text{K.E.}_{\text{rot. sail}} &= 1/2 I \omega^2 = 1/2 (1/2 M_s R_s^2) \frac{V_{SPIN}^2}{R_s^2} = \\ &= 1/4 M_s V_{SPIN}^2 \end{aligned} \quad (17)$$

in which ω is the sail's angular velocity. For a sail radius of 100 km, the minimum mass sail (no curvature) constructed of the thinnest possible material, has a mass $\approx 4 \times 10^5$ kg. Thus, since $V_{SPIN} = 0.03$ m/sec, we obtain $\text{K.E.}_{\text{rot. sail}} = 10^{12}$ joule. Therefore, a substantial amount of energy must be stored in the sail's rotation before it is released from the occulter.

Unless the sail is despun after deployment at a rotational power dissipation rate of 10^8 - 10^9 watts, the sail must be strong enough to support unbalanced sail rotation. The maximum unbalanced radial stress across the sail can be written:

$$\bar{\sigma}_u = \frac{M_s V_{SPIN}^2 / R_s}{2\pi t R_g} \quad (18)$$

where t is sail thickness and $R_g = 0.7 R_s$ for a circular sail [16]. Substituting $M_s V_{SPIN}^2 / R_s = M_s V_{sA}$, $M_s = \rho_c t \pi R_s^2$, where ρ_c is sail material density, and $R_g = 0.7 R_s$, we obtain $\bar{\sigma}_u = 0.7 \rho_s V_{sA}$. For the case $V_{sA} = 10^2$ m/sec², and $R_s = 10^5$ m, $\bar{\sigma}_u = 7 \times 10^{10} \rho_s$. For a diamond sail $\rho_s = 3.52 \times 10^3$ kg/m³, and $\bar{\sigma}_u = 2.5 \times 10^{10}$ Newton/m².

A diamond sail therefore has about two times the required tensile strength, but use of a diamond sail would increase the minimum value of $\bar{\sigma}_s$ well above 1.18×10^3 kg/m³. Also, as discussed later on, some micro-meteorite impacts are unavoidable as the sail rapidly traverses the inner Solar System. These might well cause local tensile strength reductions in the rapidly spinning sail. An alternative to spinning the sail is to tilt it inward, as shown in Fig. 6. In Figure 6, angle Θ represents the angle between the line-of-sight to the Sun and the component of solar pressure normal to the sail, $F_{S,N}$, and $F_{R'}$, is the component of solar pressure radial to the sail, directed outward from the solar sail's centre. For $F_{S,N}$, and $F_{R'}$, $\Theta = 45$ and the solar sail's area (and hence mass) is up by a factor of two from an equivalent disk shaped sail with radius R_s . Although this approach is more mass conservative than sail spin, the two are not mutually exclusive.

As the solar sail moves out from the Sun, the solar radiation pressure decreases as r^2 and the tension in the central cable c^- connecting the cable centre to payload can be gradually reduced, causing Θ to decrease.

Because the solar sail is a thin spherical shell under uniform internal (solar) pressure, the effects of membrane stress must be considered as well [17]. If the solar pressure normal to the sail is $F_{S,N}$, R_c is the sail radius of curvature (Fig. 7), and t is sail material thickness, membrane stress can be calculated:

$$\bar{\sigma}_M = \frac{F_{S,N} R_c}{8 t} \quad (19)$$

We envision an interconnected network of load carrying fibres on the spaceward side of the solar sail. If we require average solar sail area elements (as delineated by the load-carrying fibres) to function for five hours without a micro-meteoroid impact, the sail area elements will be $6.3 \times 10^{-3} \text{ m}^2$. A square fibre area element would require fibres spaced 0.08 m apart (Fig. 8).

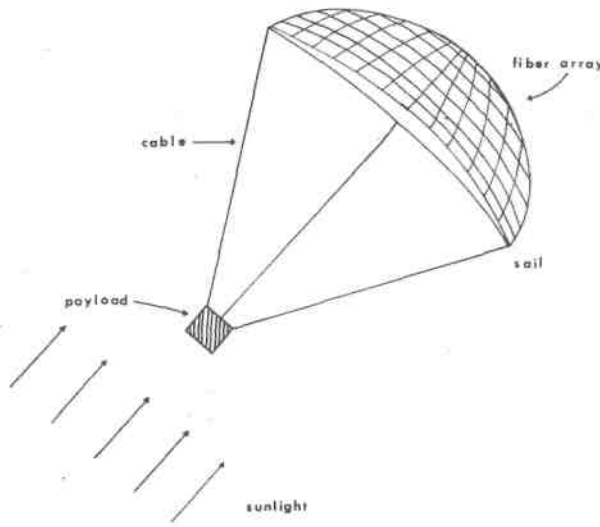


Fig. 8. A Network of Load Carrying Fibres Preceding a Fully Deployed Sail, for Micrometeoroid Protection.

The number of fibres can be written $50 R_s$ (m), for an 0.08 m fibre separation where R_s (m) is the sail radius in metres. If we use fibre such as those proposed by Forward, with a density of $2. \times 10^{-3} \text{ kg/m}^3$ and a diameter of 10^{-5} m [19] and place the fibres along the spaceward side of a fully deployed circular solar sail, as shown in Fig. 8, the total mass of the fibres can be written:

$$M_F = 1.24 \times 10^{-5} R_s^2(m) \text{ kg.} \quad (21)$$

The fibres add less than 35% to the mass of the thinnest feasible sail.

There are a total of $[25 R_s (m)]^2$ sail area elements. A 40 km radius sail therefore has 10^{12} area elements. If the total spacecraft mass is $5 \times 10^6 \text{ kg}$ and the maximum acceleration is $25 g_{\text{earth}}$ (both overestimates), the force on each area element will be 1.23×10^3 Newtons.

If we assume that all the force on a sail area element must be supported by only one of the adjacent fibres, the stress on the fibre produced by spacecraft acceleration will be 1.54×10^3 Newtons/m². Since Forward's fibres can withstand 3×10^8 Newtons/m², we are safe by several orders of magnitude [19].

Assuming instead that all the force of the sail against the fibre array must be supported by the sail area element, the stress produced on the sail area element will be 0.2 Newton/m^2 which is within reach of commercially manufactured thin film plastics, let alone the much stronger space manufactured solar sails which have here been assumed to have tensile strengths of 10^{10} to $5.3 \times 10^{10} \text{ Newton/m}^2$.

Stress problems do not seem insurmountable, although they somewhat degrade sail optimum performance. We next consider multiple aspects of mission design and sail deployment strategy.

4. PRELIMINARY MISSION DESIGN AND SOLAR SAIL DEPLOYMENT STRATEGY

The hostile thermal environment 0.01 AU from the Sun's centre will be a challenge to mission designers. A flat sail 0.01 AU from the Sun's centre and pointed toward the Sun will

receive 1×10^7 watt/m². Since both sides of a flat sail can radiate a fully absorbing (black body) sail will have a temperature of 3100 K. If 90% of the solar energy is reflected by the sail, the sail temperature at perihelion will be 1750°K. Sails with 95% and 99% reflectivities will have perihelion temperatures of 1500° K and 1100°K respectively [20]. Sail coatings reflecting 95% or more of the incident solar flux do not seem unreasonable [21]. A curved, inward-bent sail will receive less solar flux normal to the sail and will, consequently, have a lower perihelion temperature. If, at perihelion, a 95% reflective sail is so aligned that 25% of the solar flux falls normally upon it, the perihelion temperatures will be less than 1100 K, a similar sail with a reflectivity of 99% will have a perihelion temperature of about 800°K.

Metallic sails will operate in the 1000-2000°K temperature range. Boron has a melting point of 2600°K and a density of 2.5×10^3 kg/m³, so a boron sail 10^{-8} m thick would have 2.1 times the mass thickness of the thinnest projected sail [22]. It may be possible to approach the ultimate projected sail somewhat closer using superstrength fibres, although current fibres do not appear to be suited to temperatures in excess of 1000°K [23].

Fortunately, the duration of the perihelion thermal pulse will be short. The slowest approach in Table 1 passes the 0.01 AU perihelion point and continues out into space at a constant velocity of 0.0014 C (420 km/Sec). After 0.5 hr of acceleration, the spacecraft will be about 2.3×10^6 km from the Sun's centre. Both solar flux and acceleration will have fallen to 44% of their peak values. The temperature of a 90% reflective flat sail, oriented normal to the Sun, will have fallen to 1450°K.

The rapidity of the perihelion pass is both an advantage and a problem. The advantage is that, in most cases, the duration and intensity of the thermal pulse will be similar to that of re-entry from Earth-orbit into the atmosphere. An ablative shield based upon current designs may be adequate for payload thermal protection.

The problem presented by the brevity of the perihelion pass is sail deployment. There is no obvious method of deploying a 1-200 km radius sail, with a mass density 1.18×10^{-5} - 1.18×10^{-4} kg/m², in a matter of minutes or seconds. During a 0.0014 C perihelion pass, a one-minute sail-deployment timing error will amount to a trajectory error of 25,000 km, which is $\sim 0.1^\circ$ angular error. On a 4 light-year journey this constitutes a miss of 441 AU, if mid-course manoeuvres are not performed.

One way of alleviating this problem is to provide the spacecraft with a "launching pad," an inert chunk of material (asteroidal rock for the launch of a mobile habitat) more massive than the spacecraft/sail, with dimensions similar to those of the sail cross-section normal to the Sun, at initial deployment and with low albedo. Such an arrangement is shown in Fig. 2. At perihelion, the starship would cast off from the launching pad, which would (in the case of no peri-Saturn manoeuvre) continue in near-parabolic orbit around the Sun. These asteroidal chunks would themselves be equipped with solar sails for orbital corrections and could serve the dual function of providing additional thermal protection for the starship as perihelion was approached. A small fraction of the occulter or launching pad's mass might be in the form of solar sails without payload. These would be released shortly ahead of the main starship and would function to sweep up meteoritic debris, thereby reducing damage to the starship's solar sail. As discussed above, the intense thermal environment near perihelion may well reduce the requirement for such an operation.

If the starship's solar sail is partially deployed at perihelion such that the ship's maximum acceleration is $6 g_{\text{earth}}$, a non-reflecting asteroidal mass with 5 times the mass of the ship would undergo acceleration of $0.6 g_{\text{earth}}$, just before sail release. Final starship velocity would be reduced by less than 5%, by the back pressure on the occulter before sail release. This effect could be compensated for by aiming the occulter for a slightly closer perihelion pass, or using a more massive occulter.

In the case of a peri-Saturn manoeuvre, which would increase the perihelion velocity to 0.002 C, the occulter will leave the Solar System. For the 0.0014 C perihelion pass, the occulter will remain in the Solar System and can be manoeuvred for service in additional missions.

After the occulter is released and the solar-sail starship begins to depart the Solar System, the solar flux will begin to fall and the area of the sail, normal to the Sun, can be increased. For most missions, the solar sail departs perihelion so that the sail's effective radius must be increased by tens of kilometres per hour. Sails deploying at this rate do not seem to present insurmountable problems.

The intense magnetic and (non-electromagnetic) radiation environment near the Sun also poses problems. Since no probe from Earth has yet performed a close flyby of the Sun, our knowledge of the outer corona is most imperfect [24]. The interplanetary magnetic field typically has a strength of 10^{-9} weber/m² at 1 AU [24]. If the solar magnetic field can be approximated by a magnetic dipole, its value at 0.01 AU will be 10^{-3} weber/m², which is about 20-30 times stronger than the field at the surface of the Earth. A thermally protected superconducting magnet will be capable, with great reserve allowance, of providing shielding against the solar magnetic field during the perihelion pass, if that should prove desirable.

TABLE 2. Payload Mass Allotment for a 1,000-Person Interstellar Colony

Torus Structure (1,000 persons, at 35 m ² /person)	2.5 x 10 ⁶ kg
Atmosphere	10 ⁶ kg
Power plant, hardware, tools	~2.0 x 10 ⁶ kg
	~5.5 x 10 ⁶ kg

Table 2 presents the structural, atmosphere, power plant, hardware, and tool allowance for a 1000 person interstellar colony (at 35 m² /person) [25]. When allowance for colonizing the target planetary system is included a payload mass of 10⁷ kg appears realistic.

To determine performance parameters for a sample mission, first consider a sail with areal mass density (including interlocked fibres) of $\sigma_s = 5 \times 10^{-5}$ kg/m² and $R_s = 50$ km. The sail mass will be 3.93×10^5 kg. We assume $M_s = M_c + M_p$ and $M_c = 2M_p$. Using Eg. (15), for diamond cables $Vs_A = 14.6 g_{\text{earth}}$ and for copper cables $Vs_A = 4.2 g_{\text{earth}}$. From Fig. 3, for 14 g_{earth} acceleration and no peri-Saturn manoeuvre, flight time to Alpha Centauri is 1000 years. With a peri-Saturn manoeuvre, the flight to Alpha-Centauri is 950 years. For a 4 g_{earth} acceleration limit, 1350 years and 1200 years are required to reach Alpha Centauri, for the respective cases of no peri-Saturn manoeuvre and a peri-Saturn manoeuvre. The payload of each solar sail is 1.3×10^5 kg, necessitating 42 solar sails for a mission payload of 5.5×10^6 kg, 76 solar sails for a 10⁷ kg mission payload.

To decrease the number of individual solar sail starships and the consequent mission complexity, consider an increase in solar sail maximum radius to $R_s = 100$ km. Ten sails are required for the 5.5×10^6 kg payload mission and the maximum acceleration, for diamond cables, is 7 g_{earth} . Without a peri-Saturn manoeuvre, the trip time to Alpha Centauri is about 1200 years, with a peri-Saturn manoeuvre it is about 1100 years.

If R_s is increased to 190 km and diamond cables are used, the maximum acceleration is 4 g_{earth} , and only 3 sails are required to launch the 5.5×10^6 kg payload mission on a flight to Alpha Centauri requiring about 1350 years without a peri-Saturn manoeuvre, 1200 years with a peri-Saturn manoeuvre. A 1000-person interstellar population is, of course, somewhat arbitrary.

Equations (11), (12) and (5) or Fig. 3 can be utilized to evaluate the effect upon performance if σ_e is reduced. If σ_e reduced from 10^{-4} to 3.73×10^{-5} kg/m², $M_s = M_c + M_p$ and $M_c = 2M_p$ as in the case discussed above, the 190 km radius sail acceleration at a maximum of 4 g_{earth} , requires less than 950 years to reach Alpha Centauri with a peri-Saturn manoeuvre, and less than 1000 years for the transit without such a manoeuvre. Eight solar sails would be required to launch a 5.5×10^6 kg payload mission.

Details of the starship trajectory after the ship passes perihelion can be investigated using the approximate kinematical equation:

$$\Delta t = -\frac{V_i}{V_s} \pm \sqrt{\frac{V_i^2}{V_s^2} + \frac{2\Delta D}{V_s}} \quad (22)$$

in which Δt is the time required for the starship to traverse a distance increment ΔD , V_i is its velocity as it starts to traverse ΔD , and V_s is the average starship acceleration within ΔD . Approximate trajectory details can be obtained by selecting narrow ΔD , calculating solar radiation pressure and gravitational accelerations all both ends of ΔD . The velocity change with each ΔD , ΔV , can be approximated $\Delta V \approx V_s \Delta t$, which allows us to obtain V_i for the next distance increment.

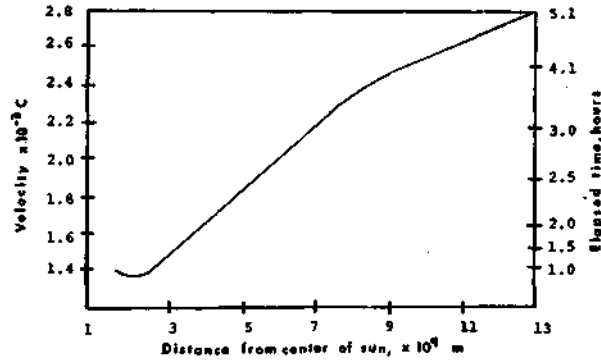


Fig. 9. Approximate Trajectory for a Solar Sail Starship with $R_s = 190$ km, $V_{sA} = 4g_{\text{earth}}$, $M = 1.13 \times 10^7$ kg, sail reflectivity = 1. The ship starts acceleration at perihelion (1.5×10^9 m) with an initial velocity of $0.0014C$. The initial velocity dip occurs because, early in the flight, solar gravitational accelerations $>$ solar radiation pressure acceleration. The sail is fully deployed and all ballast mass has been released 3.1 hr after perihelion.

Figure 9 presents kinematical details for the slowest star-ship discussed above, with $R_s = 190$ km, $V_{sA} = 4g_{\text{earth}}$, $M = 1.13 \times 10^7$ kg, $M = 1.13 \times 10^7$ kg, $r_o = 1.5 \times 10^9$ m, $V_o = 0.0014 C$, and a sail reflectivity of 1.00. Although most starship acceleration is complete after an elapsed time of 5 hours, for optimum performance it may be necessary to increase the fraction of sail mass in the form of interlocked fibres, and thereby reduce micrometeoroid degradation. If the fibre mass allotment is increased to 33% of the total sail mass, the sail will have a half-life of 10 hours and the sail material's areal mass density will be 3.35×10^{-5} kg/m².

It is useful that payload mass is only a small fraction (here 20%) of the total mass departing perihelion. Sail and cable should be retained in interstellar space and wound around the payload to protect against interstellar cosmic rays.

At a 0.01 AU perihelion, a fully deployed sail with $\sigma_e \approx 1.2 \times 10^{-4}$ kg/m² accelerates at $76 g_{\text{earth}}$ (Table 1). To keep initial acceleration less than $13 g_{\text{earth}}$, sail tilt and curvature could be supplemented by ballast mass concentric to the payload and connected by cables to the sail. This mass could serve the dual function of solar cosmic ray shielding during the perihelion pass and would be removed gradually with its cables, as the spacecraft accelerated outward.

In a multi-sail mission, solar sails might be connected in a "necklace" or "hairnet" configuration. Or, alternatively, some auxiliary drive could be utilized to allow individual sails to rendezvous.

Auxiliary propulsion for course correction, module rendezvous, and additional acceleration could be provided during the outbound leg of the trajectory using a modest technology such as the solar electric drive or mass driver [26]. A 1 course correction (for a 10 minute sail-release timing error) amounts to a velocity increment of $\sim 0.02 V$, about 25 km/sec.

5. INTERSTELLAR CRUISE AND DECELERATION

The kinetic energy of a large starship moving at even modest interstellar velocities is enormous. A 5×10^7 kg craft moving at 0.003 C or 0.004 C is 2.03×10^{19} or 3.6×10^{19} Joules, respectively. The energy of the lower velocity ship is enough to supply 5×10^8 watts of power to a human crew, if tapped continuously during a 1300 year voyage. If the initial velocity is only reduced by 7% during the interstellar cruise and if 15% of the resulting energy is efficiently used for the crew's support, 10^7 watts are available. Thus, a 1000 person population could be supported at a per capita energy level of 10 kW in this manner. Sunlight focused on the ship by the combined 350 km radius solar sails could provide this energy (at 30% conversion efficiency) only out to 4000 AU from the Sun (0.06 light year). Possible methods of obtaining on-board power from the ship's kinetic energy have been described in Refs.15 and 22.

As well as providing an on-board power source, a superconducting magnetic scoop and boron sail offer a means of mid-course trajectory control [22]. By adjusting the boron sail angle as shown in Fig. 10 and using the scoop and sail to decelerate the spacecraft by 10% of its cruise velocity, course corrections of a few degrees become possible.

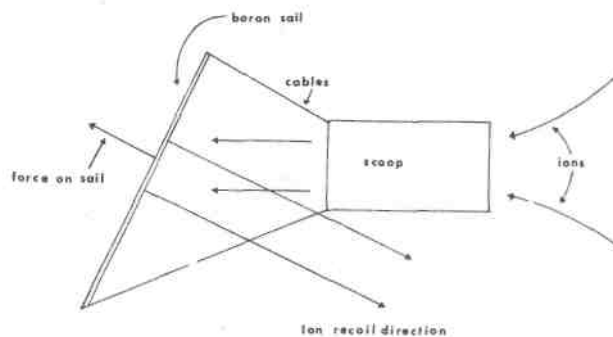


Fig. 10. Mid-course Correction Using Magnetic Scoop and Boron Deceleration Sail.

Most of the deceleration at the target solar system occurs in two stages. First, a few tenths of a light year from the target system, an electrostatic sail is used to decelerate the spacecraft to < 0.001 C. For the final stages of deceleration, the solar sail is partially unfurled. Because ion-sail collisions for the electrostatic sail in Ref. 27 are elastic, and field radii of $\sim 3 \times 10^5$ km are reasonable, deceleration at 0.003 C can be as high as 0.7 m/sec^2 . At 0.001 C, deceleration is 0.08 m/sec^2 . The solar sail need only be used during the very final deceleration stages and for manoeuvres within the target planetary system.

6. CONCLUSIONS

The near-future prospect of launching advanced solar-sail star probes at velocities as high as 0.01 C is most intriguing. Although peak velocities for solar-sail launched robot probes are less than 10% as high as those of fusion-boosted probes, the cost of solar-sail starships is likely to be many orders of magnitude less. Prospects for such probes are further discussed in the Appendix and in a recent paper by Jaffe et al [28], who expect perihelion temperatures to be 20% higher than those projected here because thin film emissivities of 0.5 might be more realisable than 1.0, as assumed here.

The reliability requirements for a centuries-long solar-sail boosted automated probe are, of course, more stringent than those for a decades long flight of a fusion boosted probe, but sail operation might be less problematic and more reliable than fusion propulsion.

For the more long-term aspects of this paper, it must be admitted that the prospect of millenia-long missions by solar-sail boosted habitats may not be attractive to terrestrials. However, long term residents of "stationary" space habitats of members of other space-faring

civilizations in the Galaxy may not feel similar constraints. Also, as Kumar has pointed out [29], there may be undiscovered stars much closer to us than Alpha Centauri, so there may be targets of opportunity only a few centuries away for inhabited starships boosted by solar sail.

Many aspects of interstellar solar sailing still remain to be optimized, such as drive selection for peri-Saturn manoeuvre (if such a manoeuvre is required) and evaluation of the advantages of additional powered flight during the inbound (post peri-Saturn) manoeuvre. Trip duration-could be shortened somewhat using a variant of Singer's pellet-stream propulsion [30]. High acceleration solar sails could launch pellet streams at velocities in excess of 0.01 C and these pellet streams could be impacted against receding sail-launched habitats.

However, it is clear that with the option of interstellar solar sailing, even in its present primitive, unoptimized state, it can be said that millenia-long interstellar missions can be launched without disrupting the economy of the agency originating the venture. Some attention should now be given to the sociological problems of maintaining a few dozen or a few hundred people for many generations between stars and to the technological problems of the cruise phase, such as the best means of obtaining and utilizing energy in interstellar space and maintaining a long-duration closed ecology.

In four to five billion years when the Sun leaves the main sequence, and the Solar System becomes less hospitable for human beings, the Sun will become a better radiation source for outgoing solar sailors. According to Novotny [31], the Sun during some phases of its red giant period would have a photosphere extending to 1 AU and its luminosity would increase by a thousandfold.

If we take Tsu's "state of the art" solar sail and enlarge it for a combined habitat-sail mass of 5×10^8 kg, the mass of the 2×10^{-3} kg/m² sail will be 4×10^8 kg and its diameter will be 500 km [9]. Peak accelerations will be gentle (~ 0.5 g) and $V_\infty \approx 0.004$ C, leaving from a circular orbit at 1 AU. An optimized sail-launched habitat should be capable of departing the Solar System of a red giant at ~ 0.01 C

Clearly, solar sail boosted interstellar probes must be seriously considered for application in the remaining decades of this millenium. For the distant future, even if our descendants develop and require more rapid methods of interstellar transport, advanced solar sails may prove to be the salavation of Solar System civilization at the time of the red giant catastrophe.

ACKNOWLEDGEMENT

G. Matloff is most grateful for discussions with Eric Drexler regarding the concept of high performance solar sails during the May 1979 Princeton Space Manufacturing Conference. G. Matloff also appreciates many discussions with Prof. M. Mautner, formerly of Rockefeller University. Computations were performed using a Texas Instruments SR52 Programmable calculator.

APPENDIX: SOLAR SAIL ROBOT INTERSTELLAR PROBES

Although the major thrust of this paper has been directed towards solar-sail launched interstellar habitats, a more immediate application of this technology might be the launch of robot interstellar probes. These could be either small versions of the interstellar habitats, with payloads suspended on cables sunward of the sail, or thin-film probes with the payload deposited as a film on the spaceward side of the sail.

In either case, since the mission would not be acceleration limited, much higher terminal velocities could be achieved than with populated missions. The peri-Saturn manoeuvre, as indicated by Eq. (5), is most significant for low V_∞ . A small probe could most likely depart directly from Earth orbit, dispensing entirely with this manoeuvre.

A typical solar-sail interstellar probe mission might proceed as follows. A sail/payload with $\sigma_e = 2 \times 10^{-5}$ kg/m² and $R_s = 10^3$ m would be constructed in near Earth orbit. The total probe mass would be 63 kg and, if the probe were directed from Earth orbit into a near-parabolic orbit

of the Sun with $V_0 = 0.01 C$, it would depart with a maximum acceleration, $V_s \text{ max}$, of $439 g_{\text{earth}}$ and achieve $V_\infty = 0.012 C$. Flight time to α Centauri would be about 350 years.

During the interstellar cruise, the 10 kg or so of payload could be used to monitor the interstellar medium; thin film optical systems could certainly be deposited on a multi-component sail. It has recently been suggested that an interstellar probe departing the Solar System could utilize the Sun's gravitational field to amplify radio emissions for stars occulted by the Sun, and act as a SETI detector [32].

To tap energy from the interstellar medium, an interstellar variation of the interplanetary Alfvén machine might be possible [33], or a superconductor-sheet such as that proposed by Matloff and Fennelly could be applied [22]. Both of these approaches would result in some spacecraft deceleration, so a thin-film radioactive-isotope battery might be considered instead.

Before departure from the Solar System, the probe would ride behind a much more massive occulter of similar dimensions. For a dark (possibly ablative occulter), occulter/sail accelerations could be limited to $0.44g_{\text{earth}}$ for an occulter mass of 3.2×10^4 kg, which is within the capability of the Space Transportation System, particularly if the shuttle external fuel tank can be orbited, ground up and incorporated into the occulter mass. Thus, the twentieth century may be capable of engineering a solar-sail launched thin-film interstellar probe requiring a few centuries to reach α Centauri.

NOMENCLATURE

A_c = cable total cross-sectional area

C = speed of light, 3×10^8 m/sec

C^- = a cable connecting the payload to the solar sail's centre

F_R = radial force on sail due to cable stress

$F_{R'}$ = solar radiation pressure component radial to sail

F_s = cable tension component balancing sunlight radiation pressure

$F_{s,n}$ = solar radiation pressure component normal to sail

F_{sun} = solar radiation pressure

g_{earth} = earth's surface gravity, 9.8 m/sec^2

G = gravitational constant 6.668×10^{-11} Newton*m²/kg²

I = moment of inertia for spinning solar sail

$K.E._{\text{rot sail}}$ = rotational kinetic energy of a spinning tail

L_c = cable length

M = combined mass of sail, cables, fibres and payload

M_c = total cable mass,

M_p = total fibre mass

M_p = payload mass

M_s = sail mass

M_\odot = solar mass, 1.989×10^{30} kg

r = radial distance from Sun centre

r_0 = radial distance from Sun centre at moment of full sail deployment

r_p = radial distance from Sun centre at perihelion

R_c = sail radius of curvature

R_g = radius of gyration for a spinning solar sail

R_s = sail effective radius cross-section, normal to Sun

$R_{s,F.S.}$ = effective radius for a fully deployed solar sail

S_r = solar irradiance at r , in watt/m²

t = sail thickness, m

T_c = cable tension

V_0 = spacecraft velocity at moment of full sail deployment

V_{CIRC} = velocity required to maintain circular orbit at r_p

V_i = velocity at start of time interval Δt

V_p = velocity at perihelion
 V_{spin} = rotational velocity of edge of spinning solar sail
 V_∞ = spacecraft departure velocity from Solar System
 V = acceleration
 V_A = maximum allowable acceleration
 V_s = average velocity during time interval at Δt
 ΔD = distance travelled during time interval Δt
 Δt = time interval during early post-perihelion acceleration
 η = cable tensile strength, Newton/m²
 θ = angle between cable and normal to the sail
 k = sail reflectivity
 ρ_c = cable density, kg/m³
 ρ_s = solar sail density
 σ_e = spacecraft effective mass thickness or areal density, kg/m²
 σ_{pa} = thin film probe areal density
 σ_s = solar sail area density
 σ_{pm} = solar sail membrane stress
 σ_u = maximum unbalanced radial stress across spinning solar sail
 \emptyset - angle between line-of-sight to Sun and $F_{s,n}$.
 ω = angular-velocity of spinning solar sail, radians/sec

REFERENCES

1. T. C. Tsu, "Interplanetary Travel by Solar Sail," ARS Journal, 29, 422-427 (1959).
2. L. D. Friedman, W. Carroll, R. Goldstein, H. Harstead, R. Jacobson, J. Kievat, R. Landel, W. Layman, E. Marsh, R. Plosza, J. Stevens, L. Stimpson, M. Trubert, G. Varsi, J. Wright, J. Hedgepath and R. MacNeal, "Solar Sailing -The Concept Made Realistic," AIAA Paper No 78-82, (1978).
3. K. E. Drexler, "High Performance Solar Sails and Related Reflecting Devices," AIAA Paper No. 79-1418; "High-Performance Solar Sail Concept," L-5 News, 4, No. 5, 7-9 (May 1979).
4. G. Marx, "Interstellar Vehicle Propelled by Terrestrial Laser Beam," Nature, 211, 22-23 (1966).
5. P. Norem, "Interstellar Travel, A Round-Trip Propulsion System with Relativistic Velocity Capabilities," AAS Paper No. 69-388(1969).
6. R. L. Forward, "Infrastellar and Interstellar Exploration," Hughes Research Report 503, September 1976.
7. D. R. J. Viewing, C J. Horswell and E. W. Palmer, "Detection of Starships, JBIS, 30, 99-104 (1977).
8. G. K. O'Neill, "The Colonization of Space," Physics Today, 27, No. 9, 32-40(1974).
9. G. L. Matloff and M. Mautner, "Solar Sails and Red Giants: The Final Fate of a Type II Civilization," presented at the 154th meeting of the American Astronomical Society, Wellesley, Mass., 11-14 June 1979, abstract in Bulletin of the American Astronomical Society, 11, No. 2,456 (1979).
10. I. S. Shlovskii and C. Sagan, Intelligent Life in the Universe, Holden-Day, San Francisco (1966).
11. K. A. Ehricke, "Saturn-Jupiter Rebound: A Method of High Speed Spacecraft Ejection from the Solar System," JBIS, 25,561-571 (1972).
12. M. R. Sharpe, Living in Space, Doubleday, Garden City, New York (1969).
13. R. W. Bucheim, Space Handbook: Astronautics and its Applications, Random House, New York (1959), pp. 138-141.

14. A. R. Martin, "Structural Limitations on Interstellar Spaceflight," *Astronautica Acta*, 16, 353-357 (1971).
15. A. L. Reimann, *Physics - Volume I*, Barnes and Noble, New York (1971) Chapt. 7.
16. G. R. Fowles, *Analytical Mechanics*, Holt, Rineholt, and Winston, New York (1962), Chapt. 8.
17. Sir R. Glazebrook, (ed.), *Dictionary of Applied Physics -Vol. 1. Mechanics, Engineering and Heat*, Peter Smith, New York (1950), p. 832.
18. W. Ley, *Rockets, Missiles and Men in Space*, Viking, New York (1968), pp. 517-518.
19. R. L. Forward, "Zero Thrust Velocity Vector Control for Interstellar Probes: Lorentz Force Navigation and Circling," *AIAA Journal*, 2, 885-889 (1964).
20. Calculations performed with a GEN-15C Radiation Calculator, as described by W. L. Wolfe, *Handbook of Military Infrared Technology*, Office of Naval Research, Dept. of the Navy, Washington, D. C (1965). Chapt. 2.
21. W. J. Smith, *Modern Optical Engineering*, McGraw-Hill, New York (1966), pp. 175-177.
22. G. L. Matloff and A. J. Fennelly, "A Superconducting Ion Scoop and Its Application to Interstellar Flight," *JBIS*, 27, 663-673 (1974).
23. J. H. Ross, "Superstrength-Fiber Applications," *Astronautics and Aeronautics*, 15, No. 12, 44-50 (1977).
24. J. C Brandt and P. W. Hodge, *Solar System Astrophysics*, McGraw-Hill, New York (1964), Chapt. 6.
25. R. D. Johnson (ed.), "Space Settlements, A Design Study," NASA SP-413, Scientific and Technical Information Service, NASA, Washington, D. C (1977), pp. 46-47.
26. G. K. O'Neill, "The Low (Profiles) Road to Space Manufacturing," *Astronautics and Aeronautics*, 16, No. 3, 24-33, (1978).
27. G. L. Matloff and A. J. Fennelly, "Interstellar Applications and Limitations of Several Electrostatic/Electromagnetic Ion Collection Techniques," *JBIS*, 30,213-222 (1977).
28. L. D. Jaffe, C Ivie, J. C Lewis, R. Lipes, H. N. Norton, J. W. Stearns, L. D. Stimpson and P. Weissman, "An Interstellar Precursor Mission," *JBIS*, 33, 3-26 (1980).
29. S. S. Kumar, "Hidden Mass in the Solar Neighbourhood" *Astrophysics and Space Science*, 17,2194-222 (1972).
30. C E.-Singer, "Interstellar Propulsion Using a Pellet Stream for Momentum Transfer," *JBIS*, 33,107-115 (1980).
31. E. Novotny, *Introduction to Stellar Atmospheres and Interiors*, Oxford, New York (1973), Chapt. 7.
32. V. R. Eshleman, "Gravitational Lens of the Sun: Its Potential for Observations and Communications over Interstellar Distances," *Science*, 205,1133-1135 (1979).
33. H. Alfve'n, "Spacecraft Propulsion'. New Methods," *Science*, 176,167-168 (1972); also see C P. Sonett, V. Fahlesonmd H. Alfven, "Electrodynamic Sailing: Beating into the Solar Wind," *Science*, 178,1115-1119 (1972).